M. SPILKA, W. ŁOŃSKI, A. RADOŃ, R. BABILAS

ISSN 0543-5846
METABK 61(3-4) 797-800 (2022)
UDC – UDK 546.621.794.72:539.26:620.193:621.9.015:620.17=111

PREPARATION AND SELECTED PROPERTIES OF $Al_{88}Y_{8-x}Fe_{4+x}$ (x = 0, 1, 2 at. %) ALLOYS IN BULK FORM

Received – Primljeno: 2021-11-04
Accepted – Prihvaćeno: 2022-03-10
Preliminary Note – Prethodno priopćenje

The paper presents selected properties of AlYFe rapidly solidified alloys. Samples in the form of plates, obtained by pressure casting method, were subjected to structural tests in order to determine the mechanical properties of the alloys, as well as their corrosion resistance. The corrosion resistance of samples was examined using polarization tests in 3,5 % NaCl solution at 25 °C. The influence of this corrosive medium on the sample's surface was analyzed with microscopic observations and energy-dispersive spectroscopy (EDS). The mechanical properties of alloys were determined by Vickers hardness tests. The results showed that the properties of $Al_{88}Y_{8-x}Fe_{4+x}$ (x = 0, 1, 2 at. %) alloys are related to changes in the content of alloying elements.

Key words: AlYFe alloys, X-ray diffraction (XRD), corrosion resistance, surface morphology changes, mechanical properties

INTRODUCTION

Metallic glasses are materials with excellent properties, such as high strength, hardness and good corrosion resistance, can be produced in various alloy systems [1, 2]. Aluminum based alloys have received special recognition for their good strength to weight ratio and corrosion resistance [3]. Alloys with a content above 80 % at. Al form a group of materials that are promising candidates for structural applications. However, the preparation of the material in the form of ribbons limits the use of these alloys, so attempts were made to produce bulk metallic glasses (BMG) [4, 5]. Unfortunately, the largest diameter of Al-rich glasses that has been obtained so far is only ~ 1 mm due to the problem of low glass forming ability (GFA) [6]. There are also no reports of the corrosive behavior of bulk aluminum-based alloys [7], and there are only findings in the literature regarding the corrosion resistance of Al-based metallic glass ribbons containing transition metals (TM) and rare earth elements (RE) [8].

Hence the aim of this work is to produce Al based metallic glasses in the form of plates, examine their structure as well as corrosion resistance and mechanical properties.

EXPERIMENTAL DETAILS

The studies were performed on $Al_{88}Y_{8-x}Fe_{4+x}$ (x = 0, 1, 2 at. %) alloys in the form of plates. The master alloy was prepared by induction melting for the appropriate mixtures of elements, such as Al (99,9 %), Y (99,9 %), Fe (99,9 %), in a ceramic crucible under argon atmosphere with technical purity (99,9 %).

The plates with a thickness of 0,5 mm were prepared by re-melting the ingots and then pressure casting. The pieces of master alloy were melted in a quartz crucible using an induction coil and cast in a copper mold by applying an ejection pressure in argon atmosphere.

The structures of melt-spun and as-cast samples of $Al_{88}Y_{8-x}Fe_{4+x}$ (x = 0, 1, 2 at. %) alloys were examined by X-ray diffraction (XRD). The phase analysis of the samples was carried out using a Rigaku Mini Flex 600, equipped with a copper tube as an X-ray radiation source and a D/TEX strip detector. The diffraction patterns were recorded by a step registration method, in the angular 2θ range, from 10° to 90°. The electrochemical corrosion investigations were conducted in 3,5 % NaCl solution at room temperature using an Autolab 302 N potentiostat, which was controlled by NOVA software (version 1.11). The measurements were performed in a three-electrode cell with a water jacket, using a saturated calomel electrode (SCE) as a reference electrode, a platinum rod as a counter electrode, and a sample as a working electrode. The corrosion resistance was evaluated by recording the open circuit potential (E_{OCP}) variation versus SCE. Corrosion current density (j_{corr}) was determined via Tafel extrapolation method using the βa and βc coefficients, and the polarization resistance (R_p) values were defined as a slope of a potential versus current density plot.

The changes of the surface morphology of the samples after electrochemical tests were analyzed using Supra 35 Carl Zeiss scanning electron microscope (SEM), combined with energy-dispersive X-ray spectroscopy (EDS), EDAX Company.

M. Spilka, e-mail: monika.spilka@polsl.pl, R. Babilas W. Łoński, A. Radoń, Silesian University of Technology, Gliwice, Poland

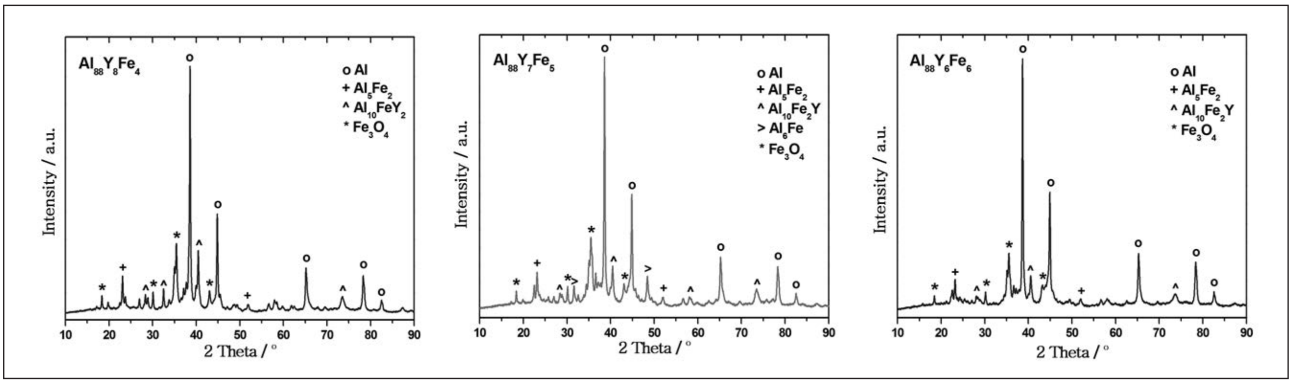

Figure 1 XRD patterns of $Al_{88}Y_6Fe_6$, $Al_{88}Y_7Fe_5$, and $Al_{88}Y_8Fe_4$ alloys in the form of plates in as-cast states

The mechanical properties of the $Al_{88}Y_{8-x}Fe_{4+x}$ (x = 0, 1, 2 at. %) alloys in the plate state were determined by conducting Vickers hardness tests using the Future-Tech FM-ARS 9000 device, under a load of 4,9 N. Twenty-five measurements were performed on each alloy studied.

RESULTS AND DISCUSSION

The structure of the Al-based alloys in the as-cast state were evaluated by X-ray diffraction (Figure 1). Alloys in the form of plates contain completely crystallized phases. The major diffraction peaks correspond to α-Al, $Al_{10}Fe_2Y$ and Al_5Fe_2 phases. Also, a presence of iron oxides was identified.

The electrochemical results obtained from measurements in 3,5 % NaCl solution at 25 °C for $Al_{88}Y_{8-x}Fe_{4+x}$ (x = 0, 1, 2 at. %) alloys in the form of plates are presented in Figure 2. It is clear that the E_{OCP} of all samples during the initial immersion time displayed unstable behavior (Figure 2a). After 3,600 s, the best E_{OCP} value was recorded for the $Al_{88}Y_8Fe_4$ alloy (-759 mV). Figure 2b shows the polarization curves of Al-Y-Fe alloys with variable content of alloying elements. Potentiodynamic studies of plate alloys (Table 1) showed a slight decrease of the corrosion potential (Ecorr), from -714 mV for the $Al_{88}Y_8Fe_4$ alloy, to -719 mV for the $Al_{88}Y_7Fe_5$ and $Al_{88}Y_6Fe_6$ alloys. The lowest value of corrosion current density (jcorr = 0,97 μA/cm^2) and the highest polarization resistance (Rp = 3,2 kΩcm^2) were obtained for the $Al_{88}Y_7Fe_5$ alloy.

Corrosion resistance properties are directly related to the structural testing results for these alloys, which is confirmed by the research carried out in [9 - 11]. Al-based amorphous alloys have a higher corrosion resistance than their crystalline counterparts [10]. The crystallized alloys are more susceptible to corrosion attack because of the occurrence of microstructural imperfections such as grain boundaries and grain edges. The formed defects create local corrosion areas, decreasing the corrosion resistance of completely crystallized alloys. The studies [11] also found that the electrochemical behavior of aluminum-rich alloys is significantly influenced by the volume fraction of the α-Al nanocrystal.

The surface morphologies of the plates after electrochemical corrosion were observed by SEM and are presented in Figure 3. The sample surfaces show residues from the corrosive medium used for the tests. EDS analysis revealed the presence of sodium, chlorine, and oxygen, which indicates that Al_2O_3, Fe_2O_3, and Y_2O_3 oxides were likely formed. The presence of metal oxides on the surface of such samples was confirmed previously [12]. In addition, SEM images did not reveal any signs of pit-

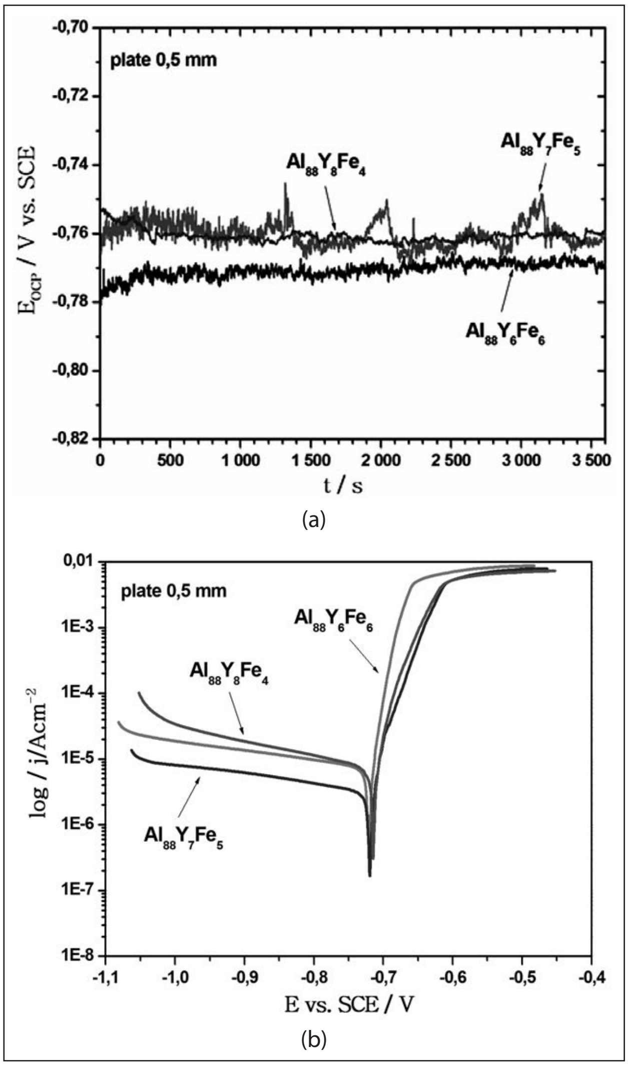

Figure 2 Variation of the open-circuit potential with time (a) and polarization curves (b) in 3,5 % NaCl solution at 25 °C of $Al_{88}Y_{8-x}Fe_{4+x}$ (x = 0, 1, 2 at. %) alloys

Table 1 **Results of polarization tests of Al-Y-Fe alloys in the form of plates (E_{OCP} = open circuit potential, E_{corr} = corrosion potential, β_a, β_c = anodic and cathodic Tafel slopes, R_p = polarization resistance, j_{corr} = corrosion current density)**

Alloy	E_{OCP} / mV	E_{corr} / mV	$\lvert\beta_a\rvert$ / mV/dec	$\lvert\beta_c\rvert$ / mV/dec	R_p / kΩcm²	j_{corr} / μA/cm²
$Al_{88}Y_{8}Fe_{4}$	-759	-714	12	8	1,7	1,27
$Al_{88}Y_{7}Fe_{5}$	-760	-719	16	12	3,2	0,97
$Al_{88}Y_{6}Fe_{6}$	-769	-719	15	6	1,3	1,53

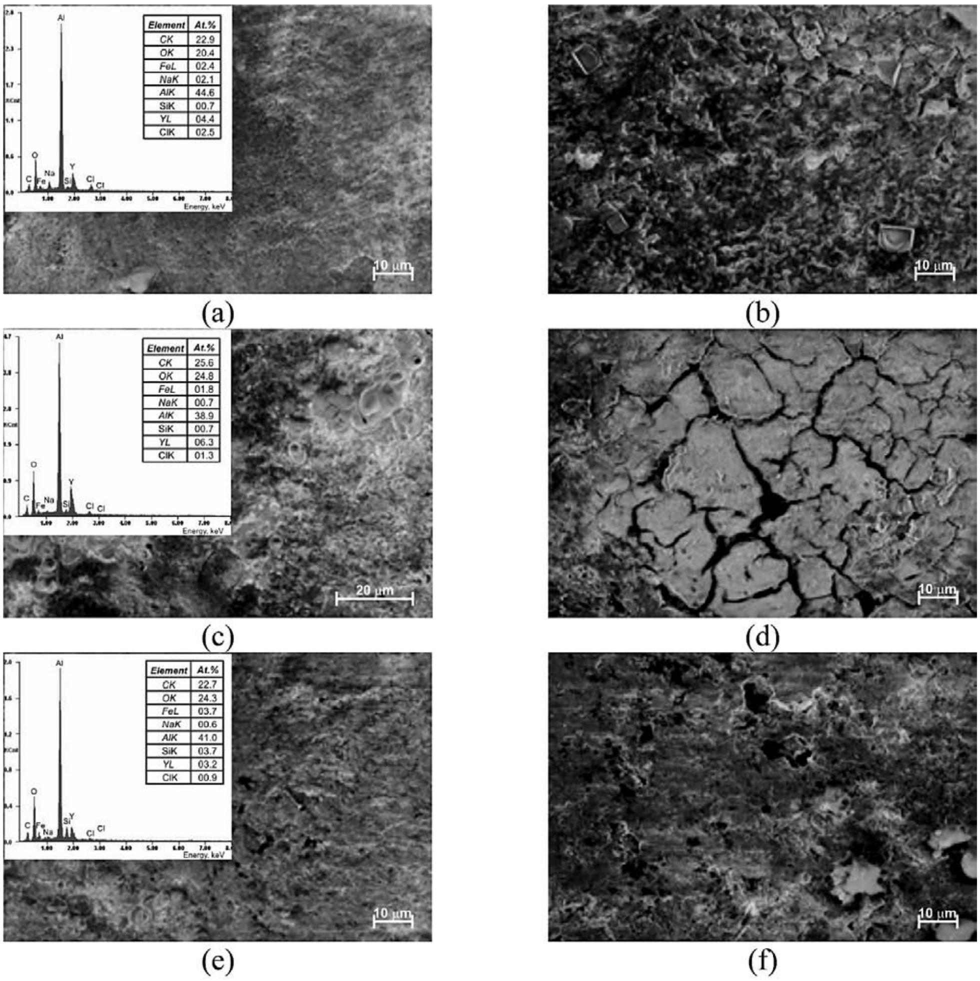

Figure 3 SEM images and EDS analysis of the surface morphology of $Al_{88}Y_{8}Fe_{4}$ (a, b), $Al_{88}Y_{7}Fe_{5}$ (c, d), and $Al_{88}Y_{6}Fe_{6}$ (e, f) alloys in the form of plates after electrochemical tests

ting, which supports the formation of a passive oxide layer on the surface and the observed corrosion resistance of these alloys in the NaCl environment.

The mechanical properties of $Al_{88}Y_{8-x}Fe_{4+x}$ (x = 0, 1, 2 at. %) alloys in the plate form, as determined by hardness tests, are presented in Table 2. The highest hardness (242 HV) was achieved for the $Al_{88}Y_{8}Fe_{4}$ alloy, which is in line with other AlYFe alloys in the literature. For example, Horimura et al. [13] found that an $Al_{90}Fe_{5}Y_{5}$ alloy in the melt-spun state had a hardness of 234 HV, and Fazakas et al. [14] reported a hardness value of 293 HV for the $Al_{88}Fe_{5}Y_{7}$ alloy in the form of a ribbon, using a 10 g load.

Table 2 **Hardness of $Al_{88}Y_{8-x}Fe_{4+x}$ (x = 0, 1, 2 at.%) alloys in the form of plates**

Alloy	HV
$Al_{88}Y_{8}Fe_{4}$	242 ± 16
$Al_{88}Y_{7}Fe_{5}$	157 ± 20
$Al_{88}Y_{6}Fe_{6}$	145 ± 31

CONCLUSIONS

X-ray diffraction investigations revealed that the studied alloys were crystalline. The alloy in the form of a plate with the lowest iron content ($Al_{88}Y_{8}Fe_{4}$) is characterized by the lowest open circuit potential (E_{OCP}) as well as the lowest corrosion potential.

The influence of alloying additives on changes in mechanical properties of AlYFe alloys in the form of plates was determined. The hardness of samples increased with increasing yttrium content, and the maximum hardness was observed for the $Al_{88}Y_{8}Fe_{4}$ alloy.

In this work interesting results have been obtained, therefore further investigations of mechanical properties and corrosion resistance of these alloys are recommended, especially in a bulk form. It is also suggested to carry out research regarding the change of properties of these alloys under the influence of annealing at different temperature, because the knowledge in this area determines the use of these materials.

Acknowledgements

The work was supported by the National Science Centre of Poland under research project no. 2018/29/B/ST8/02264.

REFERENCES

[1] C. Fan, X. Yue, A. Inoue, C-T. Liu, X. Shen, P.K. Liaw, Recent topics on the structure and crystallization of Al-based glassy alloys, Materials Research 22 (2019) 1, e20180619.

[2] X. Liang, C. Fan, J. Fu, Z. Liu, Z. Zhang, S. Ren, W. Ruan, H. Shi, Improve the forming ability of Al-based metallic glass under ultrasonic vibration at room temperature, Frontiers in Materials 8 (2021) 746955.

[3] N. Sohrabi, J. Jhabvala, R.E. Logé, Additive manufacturing of bulk metallic glasses – process, challenges and properties: A review, Metals 11 (2021) 1279.

[4] Z.P. Chen, J.E. Gao, Y. Wu, H. Wang, X.J. Liu, Z.P. Lu, Designing novel bulk metallic glass composites with a high aluminum content, Scientific Reports 3 (2013) 3353.

[5] J. Yin, H. Cai, X. Cheng, X. Zhang, Al-based bulk metallic glass with large plasticity and ultrahigh strength, Journal of Alloys and Compounds 648 (2015) 276-279.

[6] N.C. Wu, L. Zuo, J.Q. Wang, E. Ma, Designing aluminum-rich bulk metallic glasses via electronic-structure-guided microalloying, Acta Materialia 108 (2016) 143-151.

[7] V. Hasannaeimi, M. Sadeghilaridjani, S. Mukherjee, Electrochemical and corrosion behavior of metallic glasses, MDPI: Basel, Switzerland, 2021.

[8] R. Babilas, M. Spilka, K. Młynarek, W. Łoński, D. Łukowiec, A. Radoń, M. Kądziołka-Gaweł, P. Gębara, Glass-forming ability and corrosion resistance of $Al_{88}Y_{8-x}Fe_{4+x}$ (x = 0, 1, 2 at.%) alloys, Materials 14 (2021) 7, 1-12.

[9] S.D. Zhang, Z.M. Wang X.C. Chang, W.L Hou, J.Q. Wang, Identyfying the role of nanoscale heterogeneities in pitting behaviour of Al-based metallic glass, Corrosion Science 53 (2011) 3007-3015.

[10] L.A. de Oliveira, M.C.L. de Oliveira, C.T. Rios, R.A. Antunes, Corrosion of $Al_{85}Ni_9Ce_6$ amorphous alloy in the first hours of immersion in 3.5-wt% NaCl solution: The role of surface chemistry, Surface and Interface Analysis 52 (2020) 50-62.

[11] J.G. Lin, J. Xu, W.W. Wang, W. Li, Electrochemical behavior of partially crystallized amorphous $Al_{86}Ni_9La_5$ alloys, Materials Science and Engineering B 176 (2011) 49-52.

[12] P.J. Yin, C.G. Jia, L.Y. Guo, H.R. Geng, Y.S. Tian, Z.H. Zhang, W.M. Wang, Effect of Au addition on intermetallics precipitation tendency and repassivation of $Al_{88}Fe_5Y_7$ glassy alloy, International Journal of Electrochemical Science 12 (2017) 1288-1305.

[13] H. Horimura, K. Okamoto, A. Inoue, Phase decomposition and mechanical properties during annealing of melt-spun Al-Fe-Y alloys, Journal of the Japan Institute of Metals and Materials 64 (2000) 108-114.

[14] E. Fazakas, S.N. Kane, K. Lazar, L.K. Varga, Mössbauer study of rapidly solidified Al-Fe based amorphous alloys, Hyperfine Interaction 189 (2009) 119-123.

Note: The responsible translator for English language is ITAMAR Group Sp. z o.o., Gliwice, Poland